Optimization of Dynamic Ramp Metering Control with Simultaneous Perturbation Stochastic Approximation

Steven I. Chien
Associate Professor
Dept. of Civil Environmental Engineering
New Jersey Institute of Technology
Newark, NJ 07102-1982
E-mail: chien@njit.edu

J. Luo
Staff Engineer, P.E.
T & M Associates.
Middletown, NJ 07748-2792
E-mail: jluo@tandmassociates.com

ABSTRACT

Congestion is always a serious problem in many transportation commuting corridors. The need to implement effective control in the corridors has long been recognized by transportation professionals. Ramp metering has been discussed as a viable control strategy on freeways in many places of the US, which may alleviate or at least reduce the delay. In this study, a dynamic ramp metering control model is developed to maximize the total throughput with simultaneous perturbation stochastic approximation (SPSA), subject to the constraints of link densities, capacities, and feasible range of metering rates. A case study for a segment of US I-80 in New Jersey is conducted, while the impact of the proposed ramp metering control on traffic behavior is simulated with CORSIM.

KEYWORDS: Ramp Metering Control, Dynamic Systems, Simulation, Optimization

1. Introduction

Heavy congestion is always observed on urban transportation corridors in peak periods, during which delay increases and the level of service deteriorates. Starting from the early 1960s, a variety of control strategies on freeways were proposed [1, 2, 3]. Ramp metering control has been regarded as one of effective traffic management strategies for alleviating congestion.

Metering control can be pre-timed, allowing vehicles to enter a freeway every few seconds, or traffic responsive, based on real-time traffic information (e.g., gaps, speeds, occupancies and queues) on the studied freeway and ramps. By releasing vehicles from entering ramps to the freeway in measured or regulated amounts, a single vehicle or a group of vehicles can smoothly merge into the traffic stream on the mainline. Thus, the flow interruption may be reduced.

Due to the potential advantages, ramp metering control strategies have been discussed for more than four decades, varying from the simplest pre-timed metering to traffic responsive metering. Lots of efforts have been paid on optimizing metering rates for individual and/or a series of ramps through dynamic metering control models, but only a few were using simulation to quantify the benefit while consider geographical constraints. Developing a dynamic metering control model to maximize capacity (or called total throughput) subject to realistic constraints (e.g. limited storage on ramps) is the major objective of this study. The simultaneous perturbation stochastic approximation (SPSA) method is introduced in this paper to optimize ramp metering rates over continuous time intervals. Simulation approach is applied to quantify the benefit of the developed model.

2. Literature Review

According to a previous study [4], appropriate implementation of ramp metering control may improve traffic efficiency (e.g., travel time; reliability; throughput; and accidents), particularly in preventing stop-and-go and erratic traffic conditions. Such improvements can be achieved by regulating vehicles from the entering ramps, and then the flow interruption may be avoided.

In a survey conducted by Piotrowicz et al [4], the mainline speed might increase 16% to 62%, while the accident rate might decrease 24% to 50%. By considering the queuing delay on the metered ramps, the average speed still increased 20%. However, performing ramp metering might alter the pattern of traffic flow entering the freeway. Due to the delay incurred by motorists waiting for access at metering sites, a portion of ramp flow might shift to other freeway entries with less delay. The majority of diverted trips were short distance trips since their wait times spent at metered ramps were relatively longer than that of long distance trips [2, 5].

A variety of models developed for ramp metering control can be categorized into four categories, including Pre-timed Linear Programming Models [1, 5, 7], Local Traffic Responsive Models [8, 9, 10, 11], System-wide Non-linear Programming Models [12, 13], and Large-scale Heuristic Models [14, 15, 16, 17]. In classic optimization of nonlinear programming problems, such as a ramp metering control problem, the gradient of the objective function with respect to the decision variables needs to be derived. However, the degree of difficulty for deriving gradient depends on the complexity of the objective function, number of decision variable, and constraints. Thus, an efficient optimization method such as SPSA is desirable. The SPSA - based method has been demonstrated its efficiency to optimize complicated problems. Detailed description of the method may be found in Spall [18, 19], Kleinman [20], and Ting et al [21].

3. Model Development

The objective function developed here is total throughput that will be maximized subject to geographical and operational constraints, such as link densities, capacities, queue length, and the boundaries of metering rates. In order to formulate the dynamic metering control model, the following assumptions are made:

- The traffic flow on the mainline is steady without incidents blocking the freeway, which can represent the steady relationship among flow, speed and density.
- Each vehicle passes through a meter separately from other vehicles based on a first-come first-released discipline.
- The average vehicle length is in 20 feet for approximating the storage capacity of the metered ramp.

A general N-segment freeway network with multiple on-ramps and off-ramps shown in Fig. 1 has been derived by Chang et al [3, 5] as shown in Eq. 1. The metering control period can be divided into a series of equal intervals. Thus, the time varying density equation of link i at interval k, called $\rho_i(k)$ can be formulated as:

$$\rho_i(k) = \rho_i(k-1) + [q_{i-1}(k) + \delta_i^{on} R_i(k) - \delta_i^{off} \theta_i(k) Q_i(k) - q_i(k)] \frac{T}{L_i l_i} \qquad \forall i \qquad (1)$$

where l_i : number of through lanes on link i;

L_i : length of link i (miles);

$q_i(k)$: traffic volume from link i to link i+1 at interval k (vph);

$Q_i(k)$: mean flow rate of link i at interval k (vph);

$R_i(k)$: metering rate of link i at interval k (vph);

T : duration of a time interval (hours);

δ_i^{on} : binary variable (1 if link i is an on-ramp; otherwise, 0);

δ_i^{off} : binary variable (1 if link i is an off-ramp; otherwise, 0); and

$\theta_i(k)$: the turning percentage of mainline flow from link i to the off-ramp at interval k (%).

Eq. 1 shows that the projected density $\rho_i(k)$ of link i at interval k is dependent on that at the previous interval denoted as $k-1$, and the entering and exiting volumes from and to ramps. The transition flow rate denoted as $q_i(k)$ can thus be approximated by using Eq. 2:

$$q_i(k) = \alpha_i(k)[1-\delta_i^{off}\theta_i(k)]Q_i(k) + [1-\alpha_i(k)][Q_{i+1}(k) - \delta_{i+1}^{on}R_{i+1}(k)] \quad \forall i \qquad (2)$$

where $\alpha_i(k)$ is the weighted factor representing the interaction between flows on links i and i+1 at interval k. A value of 0.5 for $\alpha_i(k)$ is used here and that indicates the influences to flows on links i and i+1 and the same, and to simplify the solution procedure. Note that $\alpha_N(k)$ is equal to 1 on link N, which is the last link of the studied network. Eq. 3 represents a density function of link 1 through N, which can be derived by substituting $q_i(k)$ obtained from Eq. 2 into Eq. 1. Thus:

$$\begin{aligned}\rho_i(k) = \rho_i(k-1) &+ \frac{T}{L_i l_i}\alpha_{i-1}(k)[1-\delta_{i-1}^{off}\theta_{i-1}(k)]Q_{i-1}(k) + \frac{T}{L_i l_i}\{1-\alpha_{i-1}(k) \\ &-\alpha_i(k) - \delta_i^{off}[1-\alpha_i(k)]\theta_i(k)\}Q_i(k) + \frac{T}{L_i l_i}[\alpha_i(k)-1]Q_{i+1}(k) \\ &+ \frac{T}{L_i l_i}\alpha_{i-1}(k)\delta_i^{on}R_i(k) + \frac{T}{L_i l_i}[1-\alpha_i(k)]\delta_{i+1}^{on}R_{i+1}(k) \qquad \forall i \qquad (3)\end{aligned}$$

where $\alpha_0(k) = \alpha_N(k) = 1$; $Q_0(k) = q_0(k)$; $\delta_0^{on} = 0$; and $\theta_0(k) = 0$. In addition, the relationship [22] among speed, flow and density can be expressed as:

$$Q_i(k) = \rho_i(k) S_i(k) \tag{4}$$

where $S_i(k)$, representing the speed of link i at interval k , can be collected by loop detectors. Note that the total traffic throughput denoted as *TTT* is the total number of vehicles discharged from exit links over the control interval. Thus, TTT can be formulated as:

$$TTT = \sum_{k=1}^{K} \left[\sum_{i=1}^{N-1} \delta_i^{off} \theta_i(k) Q_i(k) + Q_N(k) \right] T \tag{5}$$

where K is the last time interval of the control period. By substituting Eq. 4 into Eq. 5, *TTT* can be derived as:

$$TTT = T \sum_{k=1}^{K} \left[\sum_{i=1}^{N-1} \delta_i^{off} \theta_i(k) \rho_i(k) S_i(k) + \rho_N(k) S_N(k) \right] \tag{6}$$

The equivalent objective function of Eq. 6 can be formulated as Eq. 7:

$$\mathbf{L}(\boldsymbol{\lambda}) = \mathbf{Z} - T \sum_{k=1}^{K} \left[\sum_{i=1}^{N-1} \delta_i^{off} \theta_i(k) \rho_i(k) S_i(k) + \rho_N(k) S_N(k) \right] \tag{7}$$

where Z represents a big number and through this conversion, the objective total throughput can be maximized by minimizing **L(λ)** subject to a set of constraints formulated in Eqs. 8, 9, and 10:

$$0 \le \rho_i(k) \le \rho^{\max} \qquad \forall i \ , k \tag{8}$$

$$0 \le Q_i(k) \le Q_i^{\max} \qquad \forall i \ , k \tag{9}$$

$$R_i^{\min} \le R_i(k) \le R_i^{\max} \qquad \forall i \ , k \tag{10}$$

Eq. 8 defines that the density of link i at interval k should be positive and less than the maximum density $\rho^{\max}$. Similarly, the flow of link i at interval k in Eq. 9 must be positive and less than the link capacity Q_i^{max}. The constraint formulated in Eq. 10 defines the range of feasible solutions, where R_i^{min} and R_i^{max} represent the lower and upper boundaries of metering rates, respectively.

Assume that vehicles approach a ramp meter with a mean arrival rate m. The relation between storage capacity denoted as L_q (called queue in number of vehicles) and metering rate $R_i(k)$ can be expressed by an M/M/1 queuing model formulated in Eq. 11. Thus,

$$L_q = \frac{\tau m}{R_i(k) - m} \tag{11}$$

where τ is the ratio of m and $R_i(k)$. Under this setting, the vehicular queue will not spillback onto the local street. R_i^{min} can be derived from Eq. 11 as:

$$R_i^{\min} = \left(\frac{L_q + \tau}{L_q} \right) m \tag{12}$$

According to a previous study [2], the maximum metering rate R_i^{max} is suggested to be 900 vph (4.0 seconds/vehicle), which considers the driver's reaction and operation time and that consumed for vehicle acceleration required a single vehicle to pass the meter.

4. The Solution Algorithm - SPSA

The SPSA algorithm, a recursive optimization technique for finding local optimizers of liner or nonlinear objective functions, was first introduced by Spall [20]. Based on the measurement of the objective function (not on the measurement of the gradient of the objective function), SPSA iteratively computes the positively and negatively perturbed objective function values. SPSA is like other Kiefer and Bolfowitz stochastic approximation algorithms, such as finite difference stochastic approximation (FDSA), in that SPSA requires only measurements (possibly noisy) of an objective function to form gradient estimates and converge to a local optimum. However, SPSA differs significantly from FDSA in requiring only two objective function evaluations per gradient estimate, whereas FDSA requires 2*p* evaluations, where *p* is the number of system parameters being estimated. This gives SPSA a significant advantage in high-dimensional problems, especially when evaluating the objective function is expensive or time-consuming [21].

The SPSA algorithm uses objective function measurements to iteratively update system control parameters until parameter values are reached that locally optimize the objective function. Let $\boldsymbol{\lambda} \in R^p$ be a vector whose components represent system parameters to be controlled, for example, the ramp metering rates and mainline traffic flow in the freeway system. Suppose **L(λ)** represents the objective function to be optimized. The goal is to find a root $\overset{*}{\lambda}_h$ of the gradient ***g*(λ)** of this objective function. That is, **λ** should be conducted from:

$$\boldsymbol{g}(\boldsymbol{\lambda}) = \frac{\partial L(\lambda)}{\partial \lambda} = 0 \qquad (13)$$

Assume that the measurement **y(λ)** of the objective function can be represented by Eq. 14 for any **λ**. Thus,

$$\mathbf{y}(\boldsymbol{\lambda}) = \mathbf{L}(\boldsymbol{\lambda}) + \mathbf{noise} \qquad (14)$$

There is no direct measurement of the gradient ***g*(λ)** that can be expressed in an equation .The SPSA algorithm gives an initial guess of the optimal **λ** represented by $\hat{\lambda}_0$ and uses **y(λ)** to update **λ** recursively until the optimal solution $\overset{*}{\lambda}_h$ is approximated. In the approximation process, SPSA produces a sequence of estimates (e.g., $\hat{\lambda}_0$, $\hat{\lambda}_1$, $\hat{\lambda}_2$, … , $\hat{\lambda}_{h+1}$) in each iteration generated by the following.

Step 0: *Initialization*

Set counter index ***h*** equal to 0. Pick initial guess $\hat{\lambda}_0$ and non-negative coefficients**, a, c, β** and **γ** in the SPSA gain sequences as shown in Eqs. 15 and 16. A large **a** enhances performance in the later iterations by producing a larger step size, while it will be effective to set **c** as some small positive number. Recommended values for β and γ are 0.602 and 0.01, respectively.

$$\mathbf{a}_h = \mathbf{a}(h + 1)^{-\beta} \tag{15}$$

$$\mathbf{c}_h = \mathbf{c}(h + 1)^{-\gamma} \tag{16}$$

Step 1: *Generate Simultaneous Perturbation Vector*

Generate a ***p***-dimensional random vector $\mathbf{\Delta}_h$ where each of the ***p*** components of $\mathbf{\Delta}_h$ is independently generated from a zero-mean probability distribution. An effective (and theoretically valid) choice for each component of $\mathbf{\Delta}_h$ is to use a Bernoulli ±1 distribution with probability of ½ for each ±1 outcome. Since uniform and normal random variables have infinite inverse moments, they are not allowed for the elements of $\mathbf{\Delta}_h$.

Step 2: *Evaluate Objective Function*

Obtain two measurements of the objective function $\mathbf{L}(\boldsymbol{\lambda})$ based on a simultaneous perturbation around the current $\hat{\lambda}_h$ (e.g., $\mathbf{y}(\hat{\lambda}_h + \mathbf{c}_h\,\mathbf{\Delta}_h)$ and $\mathbf{y}(\hat{\lambda}_h - \mathbf{c}_h\,\mathbf{\Delta}_h)$) with the $\mathbf{c}_h$ and $\mathbf{\Delta}_h$ obtained from Steps 0 and 1, respectively.

Step 3: *Approximate Gradient*

Generate the simultaneous perturbation approximation to the (unknown) ***p***-dimensional gradient as

$$\hat{g}(\hat{\lambda}_h) = \begin{bmatrix} \dfrac{\mathbf{y}(\hat{\lambda}_h + \mathbf{c}_h \boldsymbol{\Delta}_h) - \mathbf{y}(\hat{\lambda}_h - \mathbf{c}_h \boldsymbol{\Delta}_h)}{\mathbf{2}\, \mathbf{c}_h \boldsymbol{\Delta}_{h1}} \\ \dfrac{\mathbf{y}(\hat{\lambda}_h + \mathbf{c}_h \boldsymbol{\Delta}_h) - \mathbf{y}(\hat{\lambda}_h - \mathbf{c}_h \boldsymbol{\Delta}_h)}{\mathbf{2}\, \mathbf{c}_h \boldsymbol{\Delta}_{h2}} \\ \vdots \\ \dfrac{\mathbf{y}(\hat{\lambda}_h + \mathbf{c}_h \boldsymbol{\Delta}_h) - \mathbf{y}(\hat{\lambda}_h - \mathbf{c}_h \boldsymbol{\Delta}_h)}{\mathbf{2}\, \mathbf{c}_h \boldsymbol{\Delta}_{hp}} \end{bmatrix} \tag{17}$$

where $\boldsymbol{\Delta}_{hi}$ is the ith component of the $\boldsymbol{\Delta}_h$ vector. In Eq. 17, the denominators change in the p components of $\hat{g}(\hat{\lambda}_h)$. The numerators indicate the simultaneous perturbation of all components of $\hat{\lambda}_h$.

Step 4: *Update* $\hat{\lambda}_h$

Use the standard stochastic approximation form

$$\hat{\lambda}_{h+1} = \hat{\lambda}_h - \mathbf{a}_h \hat{g}(\hat{\lambda}_h) \tag{18}$$

and update $\hat{\lambda}_h$ to a new value $\hat{\lambda}_{h+1}$.

Step 5: *Iteration or Termination*

Return to **Step 1** and increase the counter index from ***h*** to ***h+1***. Terminate the algorithm if the difference between successive iterations is less than a pre-set value that is very small to approximate zero; and the last $\hat{\lambda}_h$ is the estimate of the optimum $\overset{*}{\lambda}_h$.

In the real world, traffic volumes feeding into a freeway network vary over space and time. The studied freeway should be modeled with dynamic and stochastic approach to mimic traffic and geometric situations. Thus, CORSIM is applied to model traffic operation, and the developed SPSA algorithm (see Fig. 2) is applied to search optimal metering rates that maximize the total throughput.

5. Case Study

The study site for testing the developed dynamic metering control model is a 12-mile route segment of eastbound I-80 in New Jersey. The segment contains seven on-ramps and five off-ramps for receiving and emitting flows spatially. The studied ramp junction in the network shown in Fig. 3 contains a three-lane 4-mile segment on the mainline with one-lane on-ramp and off-ramp, and a meter is located at Node 307.

CORSIM, a microscopic corridor traffic simulator developed by Federal Highway Administration (FHWA), is applied for emulating traffic operation and evaluating the developed control model. CORSIM has been used extensively to wide variety of areas by both practitioners and researchers and is one of the most wildly used traffic simulation models.

Considering dynamic system control and real-time application, time dependent demand over a series of time intervals (16 time intervals with 3-min per interval) is designed and simulated with CORSIM. In order to quantify the benefits under different conditions, various demand distributions are considered in the following cases:

- Case 1 Exiting Traffic Condition (See Table 1)
- Case 2 Increase the Entry Flow but Fix the Ramp Flow

- Case 3 Fix the Entry Flow but Increase the Ramp Flow
- Case 4 Fix both the Entry and Ramp Flows

The time-varying results of delays and throughput for Case 1 with and without metering control are shown in Fig. 4. The maximum benefit of total throughput is found of 6.2% at the fifth time interval, while the total delay is found of 3 % at the fourth time interval after the implementation of proposed metering control. There is almost no benefit under light demand condition. For Case 2, the results show that the total throughput increases from the 3rd to the 9th time interval (see Fig. 5), while the total delay may be reduced during the period between the 8th and 15th time intervals. The maximum achieved delay is 6.17% below that in Case 1. Results also showed that the developed model is efficient specifically when the entry flow ranges between 3360 vph (vehicle per hour) and 4560 vph with fixed ramp flow of 489 vph.

In Case 3, the developed control model performed well and the throughput was found increasing as demand of the ramp ranges between 373 vph and 579 vph (see Fig. 6). Meanwhile, the delay benefit is found from the 1st to 12th intervals. It indicates that the total delay may decrease before the traffic reaches the saturated condition. Finally in Case 4, the impacts of ramp storage capacity (number of queuing vehicles) to the total delay and throughput are investigated. Fig. 7 shows that the total throughput may be increased as the ramp storage capacity increases. However, the ratio of increased throughput and storage capacity may decrease as the length of the ramp exceeds the threshold point. Thus, the effectiveness of increasing total throughput subject to costly expansion of storage capacity should be evaluated.

6. Conclusions

The optimal metering rate depends on the relationship among upstream demand, downstream capacity, and the traffic volume entering the freeway from the ramp. As the analyses conducted in this study, the SPSA algorithm has been applied to optimize the ramp metering control problem subject to the queue storage area on ramps and time varying traffic condition. The total throughput can be increased without significantly increasing the delay. The benefit of applying the developed dynamic ramp metering control model has been compared other control strategies, such as Speed Control, Demand/Capacity Control, and Gap Acceptance Control. Results were summarized in a project report [23]. It was found that the developed model outperformed the control strategies listed above. Further research of this study includes:

- Conduct Benchmark-type analysis for evaluating the performance of the developed model and other demand responsive models,
- Collect real world data to calibrate the developed simulation model for testing the effectiveness and efficiency of the developed model, and
- Develop an enhanced model to optimize metering rate for multiple on-ramps in a corridors and/or a network.

References

[1]. J. A. Wattleworth, Peak-Period Analysis and Control of a Freeway System. Highway, *Research Record 157*, 1967, pp. 1-11

[2]. D. P. Masher, D. W. Ross, P. J. Wong, P. Tuan, H. M. Zeidler, & S. Petracek, *Guidelines for Design and Operation of Ramp Control Systems, National Cooperative Highway Research Program*, 1975, pp. 3-22

[3]. G. Chang, J. Wu, & H. Lieu, A Real-Time Incident-responsive System for Corridor Control: A Modeling Framework and Preliminary Results, Presented at *the 73rd Annual Meeting*, Transportation Research Board, 1994

[4]. G. Piotrowicz, & J. Robinson, Ramp Metering Status in North America, *FHWA DOT-T-95-17*, 1995

[5]. G. Chang, J. Wu, & S. L. Cohen, Integrated Real-Time Ramp Metering Model for Non-recurrent Congestion: Framework and Preliminary Results, *Transportation Research Record 1446*, TRB, 1994, pp. 56-65

[6]. C. I. Chen, J. B. Cruz, & J. G. Paquet, *Entrance Ramp Control for Travel-Rate Maximization in Expressways*. Transportation Research 8, 1974, pp.503-508

[7]. L. Chu, H. Liu, W. Recker, & M. Zhang, *Performance Evaluation of Adaptive Ramp-metering Algorithm Using Microscopic Traffic Simulation Model*, Journal of Transportation Engineering, ASCE, Vol. 130, No. 3, 2004, pp.330-338

[8]. D. R. Drew, *Gap Acceptance Characteristics for Ramp-Freeway surveillance and Control*. Highway Research Board 157, 1967, pp.108-143

[9]. N. B. Goldstein, & K. S. P. Kumar, *A Decentralized Control Strategy for Freeway Regulation*. Transportation Research 16B, 1982, pp.279-290

[10]. H. Hadj-Salem, & M. Papageorgiou, *Ramp Metering Impact on Urban Corridor Traffic, Field Results*. Transportation Research 29A, 1995, pp.303-319

[11]. J. R. McDonnell, D. B. Fogel, C. R. Rindt, W. Recker, & L. J. Fogel, *Using Evolutionary Programming to Control Metering Rates on Freeway Ramps*. J. Biethan and V. Nissen eds., Springer, Berlin, 1995, pp. 305-327

[12]. M. Papageorgiou, A New Approach to Time-of-Day Control Based on a Dynamic Freeway Traffic Model. Transportation Research 14B, 1980, pp.349-360

[13]. M. Papageorgiou, H. Hadj-Salem, & J. M. Blosseville, ALINEA: a Local Feedback Control Law for On-Ramp Metering. Transportation Research Record 1320, 1991, pp.58-64

[14]. Y. J. Stephanedes, & Chang, K. K. *Optimal Control of Freeway Corridors*. Journal of Transportation Engineering, 1993, Vol. 119, No. 4, pp.504-515

[15]. C. Taylor, D. Meldrum, & L. Jacobson, *Fuzzy Ramp Metering: Design Overview and Simulation Results*. Transportation Research Record 1634, 1998, pp.10-18

[16]. R. Wiener, L. J. Pignataro, & H. N. Yagoda, *A Discrete Markov Renewal Model of a Gap-Acceptance Entrance Ramp Controller for Expressways*. Transportation Research 4, 1970, pp.151-161

[17]. L. S. Yuan, & J. B. Kreer, *Adjustment of Freeway Ramp Metering Rates to Balance Entrance Ramp Queues*. Transportation Research 5, 1971, pp.127-133

[18]. J. C. Spall, Multivariate Stochastic Approximation Using a Simultaneous Perturbation Gradient Approximation, *IEEE,* 1992, pp.332-341

[19]. J. C. Spall, An Overview of the Simultaneous Perturbation Method for Efficient Optimization, *Airport Modeling and Simulation*, 1998, pp.141-153

[20]. N. L. Kleinman, S. D. Hill, & V. A. Ilenda, SPSA/ SIMMOD Optimization of Air Traffic Delay Cost, *Airport Modeling and Simulation*, 1998, pp.45-63

[21]. C. Ting, & P. Schonfeld, Optimization through Simulation of Waterway Transportation Investments, *Transportation Research Record 1620*, 1998, pp.11-16

[22]. A. D. May, *Traffic Flow Fundamentals*. Prentice Hall, Englewood Cliffs, N. J., 1990, pp. 238-245

[23]. S. I. Chien, & J. Luo, "Evaluation Ramp Metering Control for I-80 ITS Showcase Corridor," *Project Report FHWA-NJ-2001-013*, New Jersey Department of Transportation & National Center for Transportation and Industrial Productivity, 2001

Table 1 Traffic Demand Distribution

Index of Time Interval*	Entry Flow (vph) at Node 301			Ramp Flow at Node 307 (vph)		
	Case1	Case2	Case3	Case1	Case2	Case3
1	1472	2960	4160	173	489	240
2	3523	3160	4160	414	489	262
3	5082	3360	4160	597	489	286
4	4446	3560	4160	523	489	313
5	3962	3760	4160	466	489	341
6	3291	3960	4160	387	489	373
7	2626	4160	4160	309	489	407
8	2429	4360	4160	286	489	445
9	2331	4560	4160	274	489	486
10	2371	4760	4160	279	489	530
11	2453	4960	4160	288	489	579
12	2553	5160	4160	300	489	633
13	2703	5360	4160	318	489	691
14	2898	5560	4160	341	489	755
15	2315	5760	4160	272	489	824
16	1769	5960	4160	208	489	900

*: The duration of each time interval is 3 minutes.

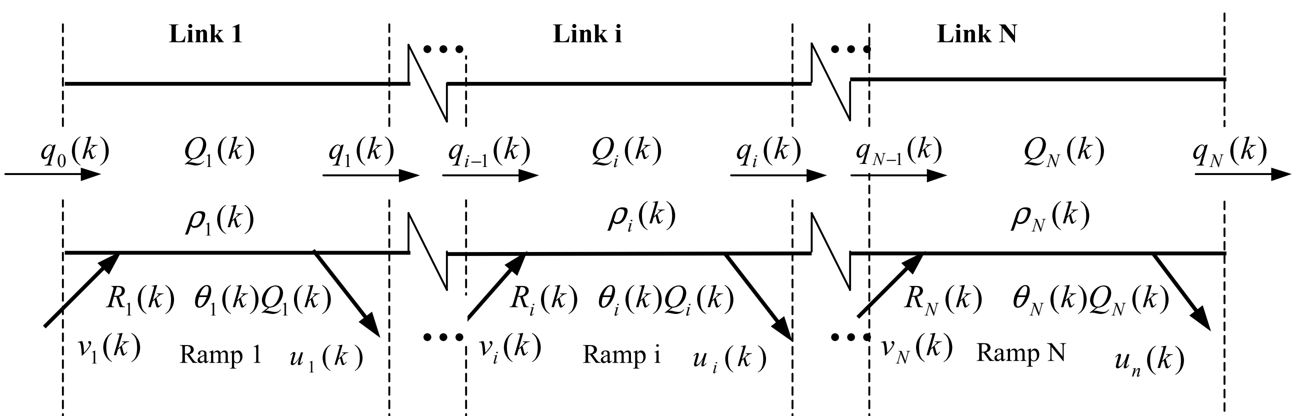

Figure 1: general freeway configuration.

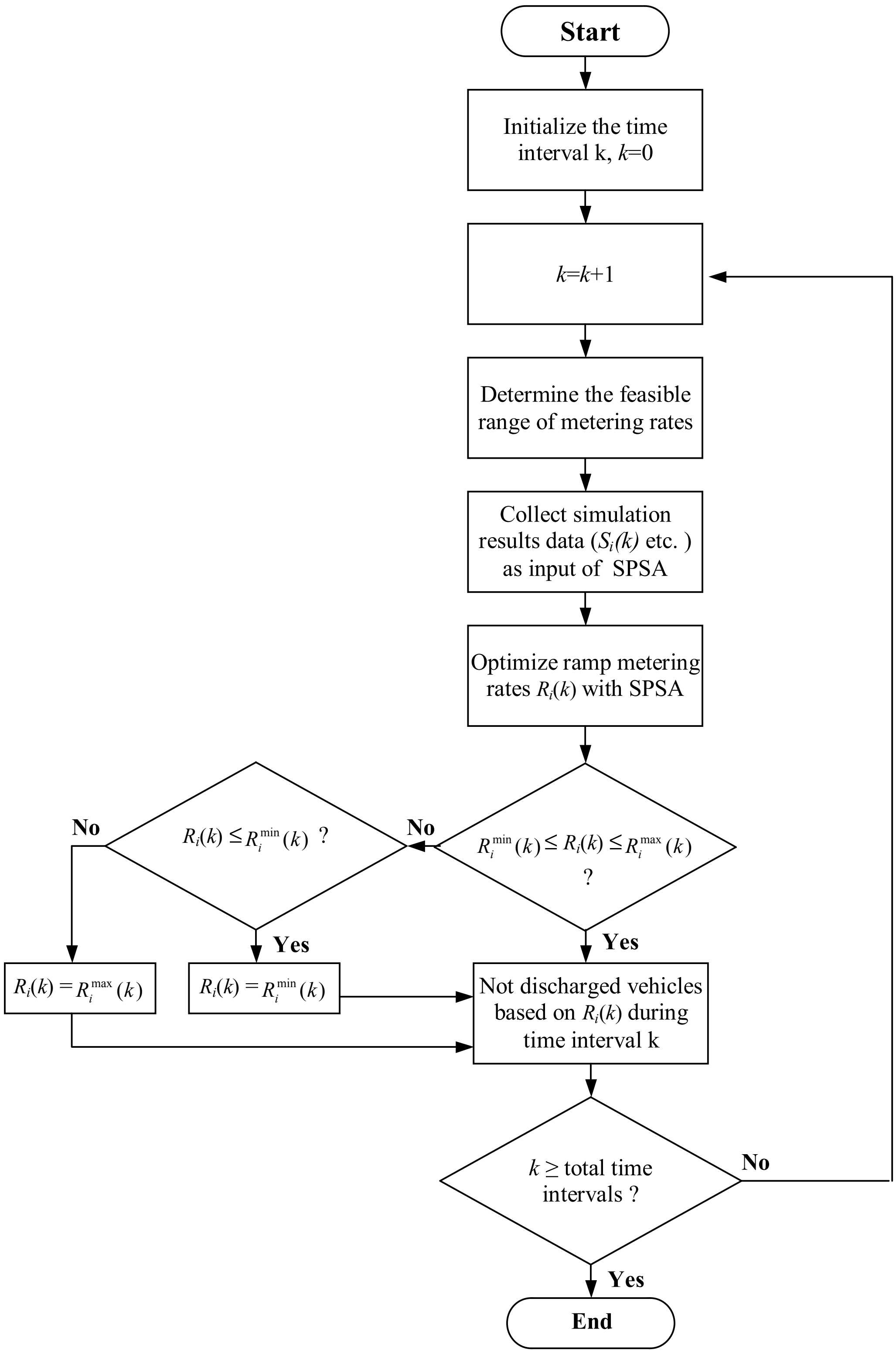

Figure 2: the real-time metering control system.

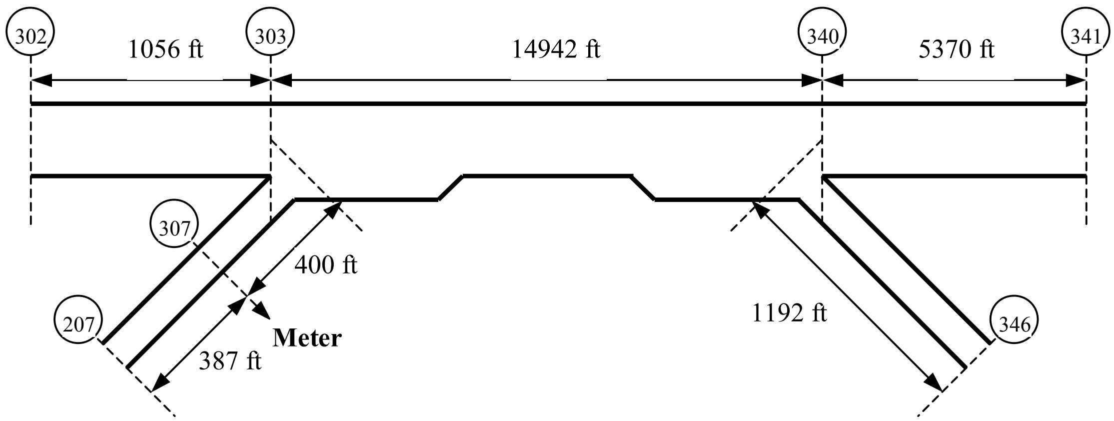

Figure 3: configuration of the study site.

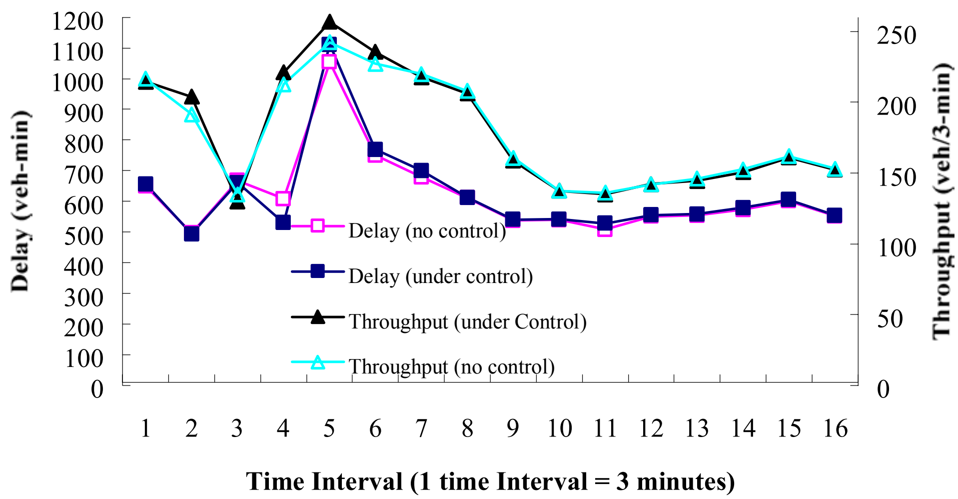

Figure 4: before and after analysis of total delay and total throughput (Case 1).

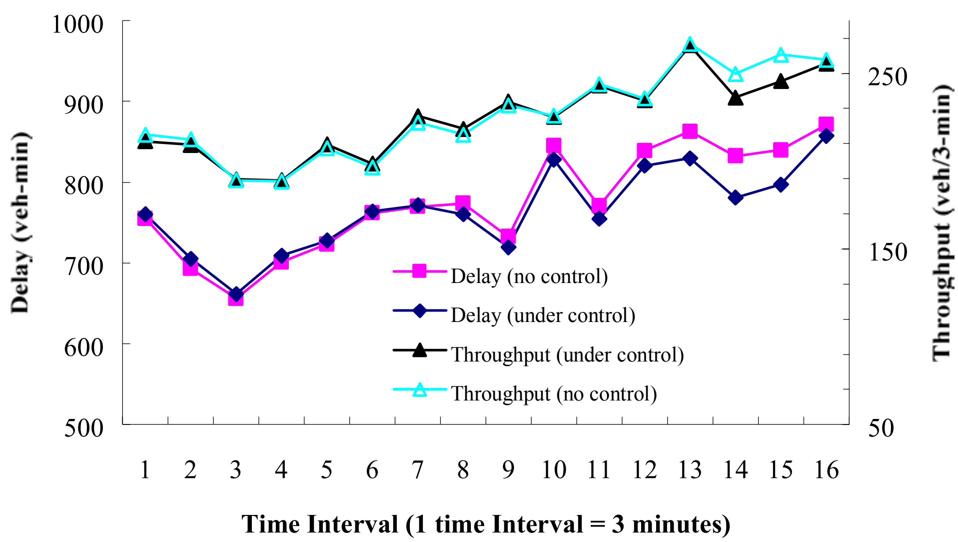

Figure 5: before and after analysis of total delay and total throughput (Case 2).

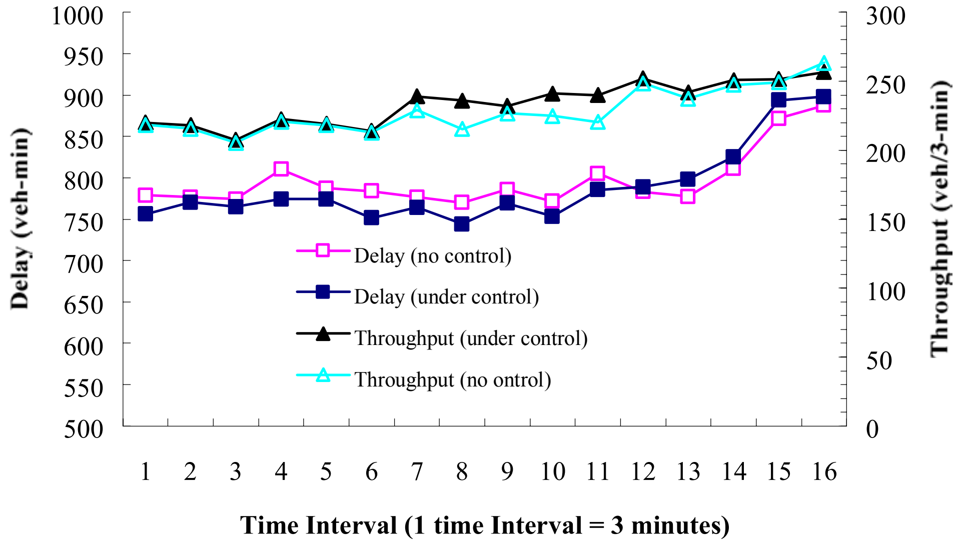

Figure 6: before and after analysis of total delay and total throughput (Case 3).

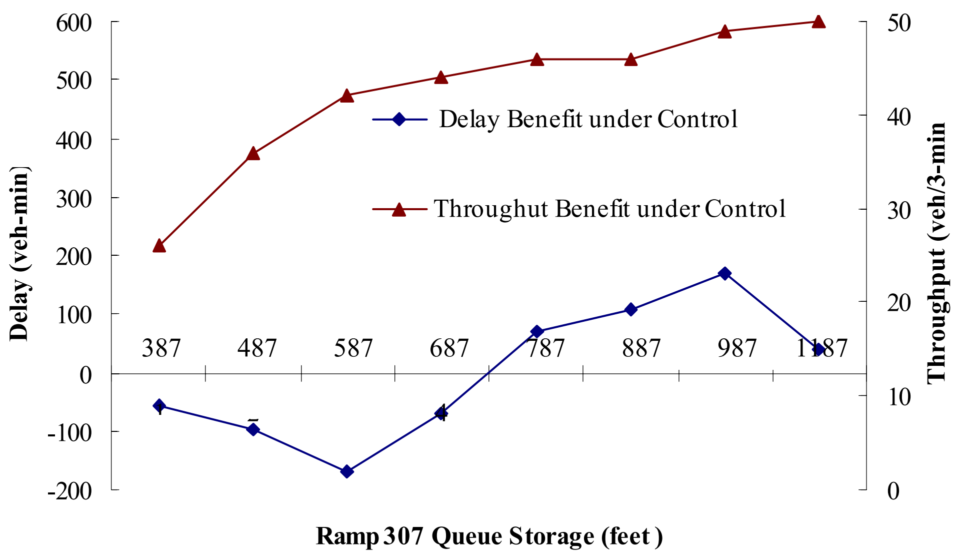

Figure 7: the benefits of total delay and total throughput (Case 4).